

# RSC Advances



This is an *Accepted Manuscript*, which has been through the Royal Society of Chemistry peer review process and has been accepted for publication.

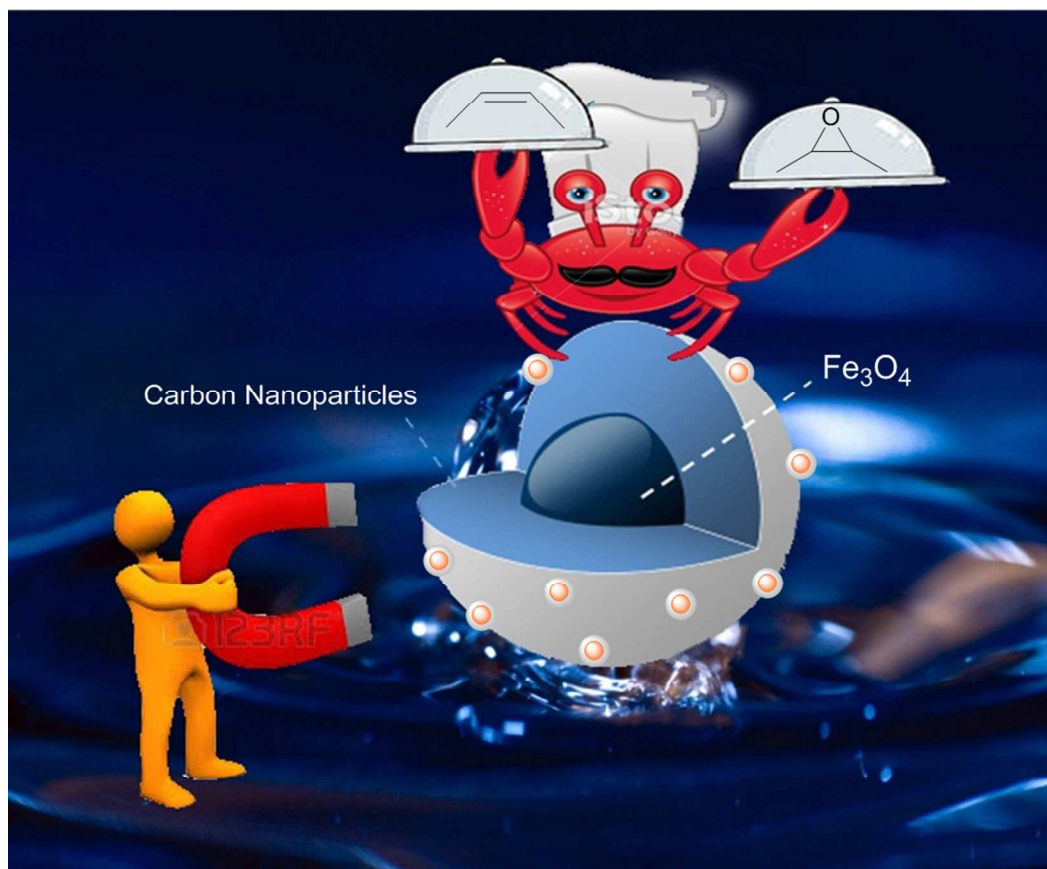
*Accepted Manuscripts* are published online shortly after acceptance, before technical editing, formatting and proof reading. Using this free service, authors can make their results available to the community, in citable form, before we publish the edited article. This *Accepted Manuscript* will be replaced by the edited, formatted and paginated article as soon as this is available.

You can find more information about *Accepted Manuscripts* in the [Information for Authors](#).

Please note that technical editing may introduce minor changes to the text and/or graphics, which may alter content. The journal's standard [Terms & Conditions](#) and the [Ethical guidelines](#) still apply. In no event shall the Royal Society of Chemistry be held responsible for any errors or omissions in this *Accepted Manuscript* or any consequences arising from the use of any information it contains.

## Graphical Abstract

### **Copper<sub>core</sub>Silver<sub>shell</sub> Nanoparticles-Yolk/Shell Fe<sub>3</sub>O<sub>4</sub>@Chitosan-Derived Carbon Nanoparticles Composite as an Efficient Catalyst for Catalytic Epoxidation on Water**



The fabrication of yolk/shell spheres consisting of a movable magnetic core, a chitosan-derived porous carbon shell, and plenty of tiny copper<sub>core</sub>silver<sub>shell</sub> nanoparticles, confined within the porous shell, is reported. The ensuing catalyst was employed for the epoxidation reaction in aqueous media at ambient temperature. The products were obtained in high yields with low amounts of the catalyst.

## ARTICLE

# Copper<sub>core</sub>Silver<sub>shell</sub> Nanoparticles-Yolk/Shell Fe<sub>3</sub>O<sub>4</sub>@Chitosan-Derived Carbon Nanoparticles Composite as an Efficient Catalyst for Catalytic Epoxidation on Water

Cite this: DOI: 10.1039/x0xx00000x

Received 00th January 2012,  
Accepted 00th January 2012

DOI: 10.1039/x0xx00000x

www.rsc.org/

Mohammad Reza Nabid\*, Yasamin Bide, and Maryam Abuali

The fabrication of yolk/shell spheres consisting of a movable magnetic core, a chitosan-derived porous carbon shell, and plenty of tiny copper<sub>core</sub>silver<sub>shell</sub> nanoparticles, confined within the porous shell, is reported. Fe<sub>3</sub>O<sub>4</sub> nanoclusters were first synthesized through solvothermal method and then SiO<sub>2</sub> shell was coated on the Fe<sub>3</sub>O<sub>4</sub> surface via a sol-gel process. Subsequently, chitosan was used to modify the surface of Fe<sub>3</sub>O<sub>4</sub>@SiO<sub>2</sub> and then, the selective etching of the middle SiO<sub>2</sub> layer was accomplished to obtain the yolk/shell Fe<sub>3</sub>O<sub>4</sub>@chitosan composites. The copper<sub>core</sub>silver<sub>shell</sub> nanoparticles immobilized on yolk/shell Fe<sub>3</sub>O<sub>4</sub>@chitosan-derived carbon nanoparticle could be synthesized starting with copper<sub>core</sub>silver<sub>shell</sub> nanoparticles-yolk/shell Fe<sub>3</sub>O<sub>4</sub>@chitosan composite; which is due to the well-known strong affinity of chitosan for transition metals. The ensuing catalyst was employed for the epoxidation reaction in aqueous media at ambient temperature. The products were obtained in high yields with low amounts of the catalyst.

## Introduction

Due to many different advantages of nanoparticles (NPs) such as the large surface-to-volume ratio and combining the characteristics of homogeneous (relatively low catalyst loadings and good selectivity) and heterogeneous catalysis (recovery and recyclability),<sup>1</sup> employing metal nanoparticles in catalysis has significantly increased recently.<sup>2</sup> However, because of the high surface area of metal clusters, they tend to aggregate into larger particles which lead to the loss of catalytic activity. Solving this problem and enhancing environmental consciousness and also promoting the efficiency of chemical reactions under benign conditions with recyclability of catalysts are the essential parts of chemical researches.<sup>3</sup> One of the best approaches to improve the efficiency and recyclability of the catalysts is their immobilization on the solid supports.<sup>4-6</sup> Among the biopolymers, chitosan (CTS) has received growing attention as a functional, non-toxic, renewable, and biocompatible polymer, which has many applications, such as metal extraction,<sup>7,9</sup> and in some recent examples as catalytic support.<sup>10,11</sup> Recent reports propose that carbon nanoparticles (CNPs), because of their stability, sizes, ease of dispersion in liquid medium and facile formation of composites, especially with catalytic metal nanoparticles, could provide better options.<sup>12-14</sup> Chitosan-derived carbon nanoparticles, because of the convenient method of synthesis, being bio-compatible, inexpensive and thermally stable, are really good candidates for stabilizing noble metals and heterogeneous catalysis. Yolk/shell nanostructures (YSNs) consisting a core encapsulated in a hollow capsule with a porous shell are

interesting family of nano-architectures. These systems have attracted considerable attention over the past few years in a variety of applications including catalysis, storage, and drug delivery due to their unique properties, such as large surface area, multi-functionality and excellent loading capacity.<sup>15-18</sup> Among them, YSNs with a magnetic core, because of the improved stability, biocompatibility, and significant magnetization strength of iron oxides are desirable in biomedical applications.<sup>19,20</sup> Also YSNs with a magnetic core and a functional shell are attractive because of their potential applications as catalyst supports and also elimination of time-consuming separation procedures such as filtration or centrifugation. On the other hand, the outer shells of yolk-shell composites usually need to have both high surface areas and good dispersion characteristics to be the catalyst support, which chitosan-derived carbon nanoparticles are excellent choices. Based on our interest in the development of sustainable benign pathways for organic transformations, and nano-catalysis,<sup>21-26</sup> we decided to synthesize copper<sub>core</sub>silver<sub>shell</sub> nanoparticles immobilized on the yolk/shell Fe<sub>3</sub>O<sub>4</sub>@chitosan-derived carbon nanoparticle and to explore their performance for catalytic epoxidation reactions "on water". The main difficulty in utilization of non-noble metals such as Co, Ni, Fe and Cu arises from their tendency toward oxidation at ambient conditions, particularly as their size gets smaller.<sup>27,28</sup> However, very high cost of silver limits its wide industrial applications as a catalyst. Since copper is much cheaper than silver but possesses a very high conductivity (only 6% less than that of Ag), Cu NPs can be considered as a replacement for silver NPs. Employing copper-silver core-shell (Cu<sub>core</sub>Ag<sub>shell</sub>) nanoparticles leads to

have the optical and electrical properties of both metals, and also prevent the oxidation of copper core.<sup>29</sup> Moreover, Cu–Ag bimetallic catalyst should be more selective than pure silver for epoxidation.<sup>30</sup>

## Experimental

### Materials

Chitosan, copper nitrate trihydrate ( $\text{Cu}(\text{NO}_3)_2 \cdot 3\text{H}_2\text{O}$ ) and silver nitrate ( $\text{AgNO}_3$ ) were purchased from Aldrich Company. Ferric chloride hexahydrate ( $\text{FeCl}_3 \cdot 6\text{H}_2\text{O}$ ), trisodium citrate dehydrate, sodium acetate (NaAc), ethylene glycol (EG), tetraethyl orthosilicate (TEOS), and sodium hydroxide (NaOH) were purchased from Merck Chem. Co. All other chemicals were purchased from Aldrich or Merck companies and used as received without any further purification.

### Instruments and characterization

Fourier transform infrared (FT-IR) spectra were recorded on a Bomem MB-Series FT-IR spectrophotometer. Transmission electron microscopy (TEM) was performed by LEO 912AB electron microscope. Ultrasonic bath (EUROSONIC® 4D ultrasound cleaner with a frequency of 50 kHz and an output power of 350 W) was used to disperse materials in solvents. Thermogravimetric (TG) and differential thermal analysis (DTA) were carried out using STA 1500 instrument at a heating rate of  $10\text{ }^\circ\text{C min}^{-1}$  in air. X-ray powder diffraction (XRD) data were collected on an XD-3A diffractometer using  $\text{Cu K}\alpha$  radiation. X-ray photoelectron spectroscopy (XPS) was performed using a VG multilab 2000 spectrometer (ThermoVG scientific) in an ultrahigh vacuum. Ultraviolet–Visible (UV-Vis) spectra were obtained using a Shimadzu UV-2100 spectrophotometer. Scanning electron microscope (SEM) and energy-dispersive x-ray spectroscopy (EDS) were performed on a Zeiss Supra 55 VP SEM instrument. Catalysis products were analyzed using a Varian 3900 gas chromatograph (GC) (conversions were obtained using toluene as an internal standard). AA-680 Shimadzu (Kyoto, Japan) flame atomic absorption spectrometer (AAS) with a deuterium background corrector was used for determination of the metals.

### Synthesis and coating of the $\text{Fe}_3\text{O}_4$ with silica

$\text{Fe}_3\text{O}_4$  nanoclusters were synthesized according to the procedure described in literature.<sup>31</sup> Typically,  $\text{FeCl}_3$  (0.65 g, 4.0 mmol) and trisodium citrate (0.20 g, 0.68 mmol) were first dissolved in ethylene glycol (20 mL). Afterward, NaAc (1.20 g) was added with stirring. The mixture was stirred vigorously for 30 min and then sealed in a Teflon-lined stainless-steel autoclave. The autoclave was heated at  $200\text{ }^\circ\text{C}$  and maintained for 10 h, and then allowed to cool to room temperature. The obtained  $\text{Fe}_3\text{O}_4$  particle suspension was washed with  $\text{H}_2\text{O}$  and EtOH three times and then dried in a vacuum oven for 12 h at room temperature. For coating of  $\text{Fe}_3\text{O}_4$  with silica, 50.0 mL as-prepared  $\text{Fe}_3\text{O}_4$  nanocluster solution (containing 0.4 g  $\text{Fe}_3\text{O}_4$ ) was dispersed into the mixture of deionized water (10.0 mL), ethanol (100.0 mL) and  $\text{NH}_3 \cdot \text{H}_2\text{O}$  (50.0 mL). After imposing to ultrasonic radiation for 10 min, a certain amount of TEOS was quickly added into the system. The reaction was allowed to proceed with stirring for 8 h at room temperature. Finally the

products were separated with magnet and washed with deionized water for the next-step.

### Preparation of the yolk-shell $\text{Fe}_3\text{O}_4$ @chitosan

To perform chitosan coating, 0.4 g of as-prepared  $\text{Fe}_3\text{O}_4$ @ $\text{SiO}_2$  core-shell NPs was mixed with 0.4 g of chitosan in 60 mL water for 3 h. The obtained  $\text{Fe}_3\text{O}_4$ @ $\text{SiO}_2$ @chitosan core-shell NPs were washed with ethanol and water for several times and dried in vacuum oven. The synthesized  $\text{Fe}_3\text{O}_4$ @ $\text{SiO}_2$ @chitosan composites were soaked in 1.0 M NaOH solution under mechanical stirring for 12.0 h. The  $\text{SiO}_2$  layer between the chitosan shell and the  $\text{Fe}_3\text{O}_4$  core was selectively etched. The black product was washed with deionized water and ethanol several times and dried in oven.

### Preparation of the yolk/shell $\text{Fe}_3\text{O}_4$ @chitosan/ $\text{Cu}_{\text{core}}\text{Ag}_{\text{shell}}$ composites

For immobilization of  $\text{Cu}_{\text{core}}\text{Ag}_{\text{shell}}$  on the yolk-shell  $\text{Fe}_3\text{O}_4$ @chitosan, in a typical procedure, 0.072 g of  $\text{Cu}(\text{NO}_3)_2 \cdot 3\text{H}_2\text{O}$  (0.3 mmol) was dissolved in 5 mL water and then 0.15 g of yolk-shell  $\text{Fe}_3\text{O}_4$ @chitosan was added to the solution. The mixture was stirred for 8 h and subsequently, 0.194 mL hydrazine hydrate (4 mmol) in 5 mL water was added. After 1 h of stirring, the solution was diluted with 100 mL of triple distilled water followed by dropwise addition of 0.1 mL (2.5 mmol) acetaldehyde. After 5 min of stirring, 0.006 g (0.036 mmol) silver nitrate was dissolved in 10 mL water and added with stirring to the above mixture. After 2 h, the product was excluded with an external magnetic field, washed with deionized water and ethanol and dried for 24 h in vacuum oven at  $50\text{ }^\circ\text{C}$ . The amounts of metals in the synthesized catalyst were measured with AAS to be 4.4% (w/w) Ag and 19.2% (w/w) Cu.

### Preparation of copper<sub>core</sub>silver<sub>shell</sub> nanoparticles immobilized on the yolk/shell $\text{Fe}_3\text{O}_4$ @chitosan-derived carbon nanoparticle

0.4 g of the  $\text{Cu}_{\text{core}}\text{Ag}_{\text{shell}}/\text{yolk/shell } \text{Fe}_3\text{O}_4$ @chitosan composites was dissolved in 12 mL 1% acetic acid solution and then the mixture was sealed into a Teflon equipped stainless steel autoclave, which was then placed in a muffle furnace followed by hydrothermal treatment at  $180\text{ }^\circ\text{C}$  for 12 h. A programmed temperature profile was adopted to control the heating process. The heating rate was set at  $5\text{ }^\circ\text{C.min}^{-1}$ . After the reaction, the autoclave was cooled down naturally. The product was magnetically separated and washed successively with deionized water, ethanol and acetone and dried at  $40\text{ }^\circ\text{C}$  for 12 h before further usage.

### General procedure for the catalytic epoxidation of alkenes

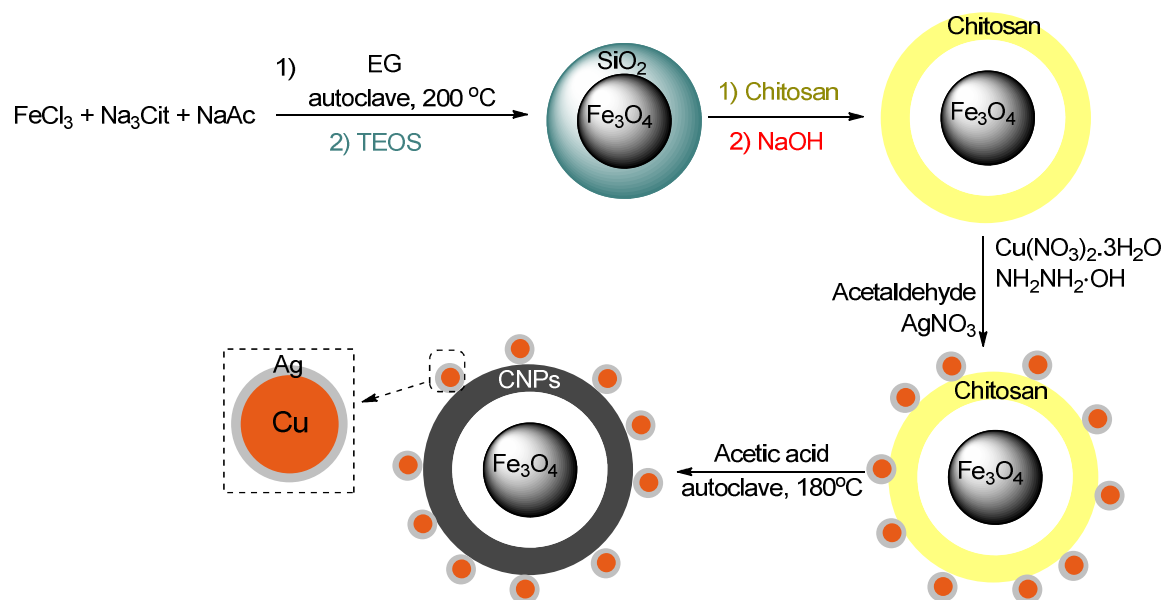
Catalytic experiments were initiated with the oxidation of styrene (0.5 mmol) with  $\text{O}_2$  (1 atm) in the presence of 0.3 mol % Cu and 0.04 mol% Ag in distilled water at  $25\text{ }^\circ\text{C}$ . It led to 17, 36, 49 and >99% conversion (obtained with GC based on toluene as internal standard) after 20, 40, 60 and 120 min, respectively. After the reaction completion, the catalyst was removed via an external magnetic field and then reused in the next cycle. The catalytic epoxidation reactions of other alkenes were conducted under the same conditions of styrene.

## Results and discussion

### Synthesis and recognition of the catalyst

The practical procedure for the synthesis of copper<sub>core</sub>silver<sub>shell</sub> nanoparticles immobilized on the yolk/shell Fe<sub>3</sub>O<sub>4</sub>@chitosan-derived carbon nanoparticle can be divided to four steps which is schematically shown in Scheme 1: (i) The magnetite particles were synthesized via a modified solvothermal reaction of FeCl<sub>3</sub> in the presence of trisodium citrate (Na<sub>3</sub>Cit) and sodium acetate at 200 °C according to procedure described by Liu et al.<sup>31</sup> Due to the strong coordination affinity of carboxylate groups of Na<sub>3</sub>Cit to Fe(III) ions, they prevents Fe(III) ions from aggregating into large particles.<sup>32</sup> Then, SiO<sub>2</sub> shell was coated on the Fe<sub>3</sub>O<sub>4</sub> nanoparticle surface through a sol-gel process to prevent coagulation of the particles and to overcome the solubility problems in organic media. Also SiO<sub>2</sub> shell is required to obtain the desired yolk-shell structure; (ii) A functional, non-toxic, and biocompatible polymer, chitosan, was used to modify the surfaces of Fe<sub>3</sub>O<sub>4</sub>@SiO<sub>2</sub> core-shell NPs. Then, the resulting Fe<sub>3</sub>O<sub>4</sub>@chitosan NPs was treated with NaOH solution which the SiO<sub>2</sub> layer was selectively etched and the yolk/shell structure with a movable Fe<sub>3</sub>O<sub>4</sub> nanoparticle inside the hollow chitosan shell was formed; (iii) The yolk/shell Fe<sub>3</sub>O<sub>4</sub>@chitosan stabilized Cu<sub>core</sub>Ag<sub>shell</sub> NPs was synthesized by a transmetalation reaction on the surface of copper nanoparticles immobilized on the yolk/shell Fe<sub>3</sub>O<sub>4</sub>@chitosan, where the copper atoms on the particles' surface are used as the reducing agent for the silver. This process leads to formation of only Cu<sub>core</sub>Ag<sub>shell</sub> NPs on the yolk/shell Fe<sub>3</sub>O<sub>4</sub>@chitosan, with no individual silver particles,<sup>29</sup> (iv) In the next step, carbon nanoparticles were obtained by hydrothermal carbonization of chitosan at a mild temperature to obtain the Cu<sub>core</sub>Ag<sub>shell</sub> NPs immobilized on the yolk/shell Fe<sub>3</sub>O<sub>4</sub>@chitosan-derived carbon nanoparticle which the method is very cheap and absolutely green.<sup>33</sup> FT-IR spectra of Fe<sub>3</sub>O<sub>4</sub> magnetic particles, Fe<sub>3</sub>O<sub>4</sub>@SiO<sub>2</sub>, Fe<sub>3</sub>O<sub>4</sub>@SiO<sub>2</sub>@chitosan, yolk-shell Fe<sub>3</sub>O<sub>4</sub>@chitosan, and Cu<sub>core</sub>Ag<sub>shell</sub>/YS-Fe<sub>3</sub>O<sub>4</sub>@(Chit.der)CNPs are shown in Fig. 1 a-e, respectively. FT-IR spectrum of the magnetite particles (Fig. 1a) shows absorption bands at 1630 and 1405 cm<sup>-1</sup> which are attributed to carboxylate, indicating the presence of carboxyl groups which is attributed to Na<sub>3</sub>Cit. The bands at 580 and 3424 cm<sup>-1</sup> are ascribed to the Fe-O

vibrating and O-H vibrating, respectively. In the spectrum of Fe<sub>3</sub>O<sub>4</sub>@SiO<sub>2</sub> composites (Fig. 1b), in addition to the absorption bands of Fe-O at 598 and 462 cm<sup>-1</sup>, the band at 1096 cm<sup>-1</sup> related to Si-O-Si stretching vibrations of SiO<sub>2</sub> shell is also seen. From Fig. 1c, for Fe<sub>3</sub>O<sub>4</sub>@SiO<sub>2</sub>@chitosan, the characteristic peaks of chitosan have been overlapped with the SiO<sub>2</sub> peaks. In the spectrum of yolk-shell Fe<sub>3</sub>O<sub>4</sub>@chitosan (Fig. 1d), the absorption peak of Si-O-Si at 1096 cm<sup>-1</sup> has been disappeared, indicating the middle SiO<sub>2</sub> shell is completely etched. Also, the C-H bending vibrations of the pyranose ring of chitosan appear at 1026-1155cm<sup>-1</sup>, which are similar to that of the pure chitosan sample confirming that the chitosan shell is successfully synthesized. The XRD spectra of Fe<sub>3</sub>O<sub>4</sub>, Fe<sub>3</sub>O<sub>4</sub>@SiO<sub>2</sub>, Fe<sub>3</sub>O<sub>4</sub>@SiO<sub>2</sub>@chitosan, yolk-shell Fe<sub>3</sub>O<sub>4</sub>@chitosan, and Cu<sub>core</sub>Ag<sub>shell</sub>/YS-Fe<sub>3</sub>O<sub>4</sub>@(Chit.der)CNPs are presented in Fig. 2a-e. In the XRD pattern of Fe<sub>3</sub>O<sub>4</sub>, six characteristic diffraction peaks at 2θ =30.27°, 35.61°, 43.29°, 57.24°, 62.84°, and 73.94° are observed which are related to (220), (311), (400), (511), (440) and (622) Bragg diffractions of face centered cubic structure of Fe<sub>3</sub>O<sub>4</sub> (Fig. 1a). The XRD pattern of Fe<sub>3</sub>O<sub>4</sub>@SiO<sub>2</sub> shows an additional broad peak at around 2θ=23.35° because of the amorphous silica shell (Fig. 2b). The pattern of Fe<sub>3</sub>O<sub>4</sub>@SiO<sub>2</sub>@chitosan presented in Fig. 2c shows two peaks of chitosan; the main reflection at 20.10° and another smaller and broader peak at 2θ = 10.52°. However, the diffraction peak of chitosan at 20.10° has been overlapped with the characteristic peak of silica shell in that region. In the XRD pattern of the yolk-shell Fe<sub>3</sub>O<sub>4</sub>@chitosan (Fig. 2d), the peak of silica at 20.10° is eliminated, as is expected due to the removing of silica intermediate shell, and therefore the diffraction peak at 19.98° is attributed to chitosan. As can be seen in the XRD pattern of Cu<sub>core</sub>Ag<sub>shell</sub>/YS-Fe<sub>3</sub>O<sub>4</sub>@(Chit.der)CNPs presented in Fig. 2e, after hydrothermal carbonization, the crystallinity of chitosan is reduced and the CNPs show a broader peak at 2θ =21.02, exhibiting an amorphous carbon phase. Moreover, the pattern shows the main diffraction peaks of both copper and silver with fcc crystal structures at 2θ values of 44.58° and 37.17°, respectively.



**Scheme 1** Schematic diagram of the synthesis of Cu<sub>core</sub>Ag<sub>shell</sub>/YS-Fe<sub>3</sub>O<sub>4</sub>@(Chit.der)CNPs.

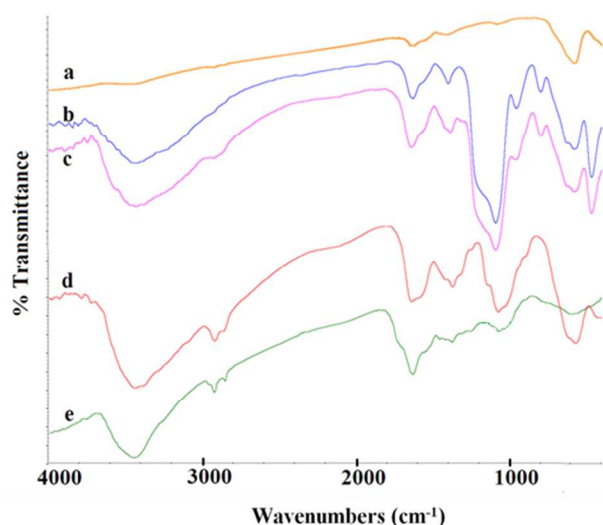


**Fig. 1** FT-IR spectra of  $\text{Fe}_3\text{O}_4$  (a),  $\text{Fe}_3\text{O}_4@SiO_2$  (b),  $\text{Fe}_3\text{O}_4@SiO_2@chitosan$  (c), yolk-shell  $\text{Fe}_3\text{O}_4@chitosan$  (d), and  $\text{Cu}_{core}\text{Ag}_{shell}/\text{YS-Fe}_3\text{O}_4@(\text{Chit.der})\text{CNPs}$  (e).

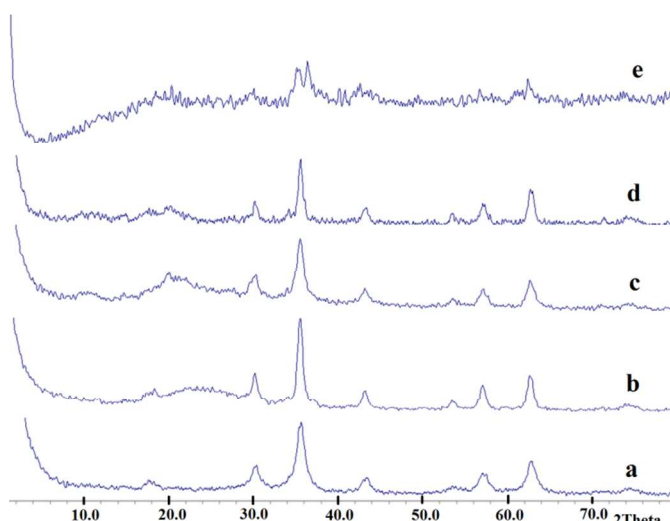


**Fig. 2** XRD patterns of  $\text{Fe}_3\text{O}_4$  (a),  $\text{Fe}_3\text{O}_4@SiO_2$  (b),  $\text{Fe}_3\text{O}_4@SiO_2@chitosan$  (c), yolk-shell  $\text{Fe}_3\text{O}_4@chitosan$  (d), and  $\text{Cu}_{core}\text{Ag}_{shell}/\text{YS-Fe}_3\text{O}_4@(\text{Chit.der})\text{CNPs}$  (e).

TGA of magnetite particles (Fig. 3a) shows a weight loss of about 6.8 wt% in the range of 100–800°C, suggesting the presence of organic species.

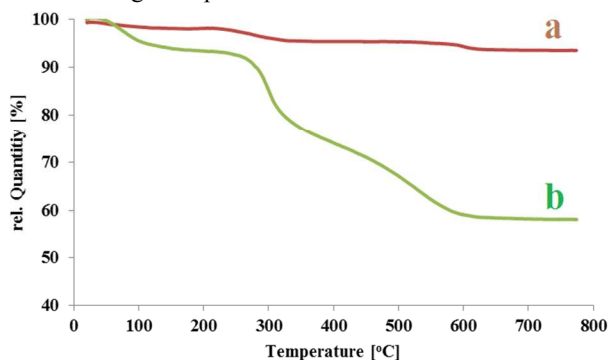


**Fig. 3** TGA curves of  $\text{Fe}_3\text{O}_4$  (a), and  $\text{Fe}_3\text{O}_4@SiO_2@chitosan$  (b).

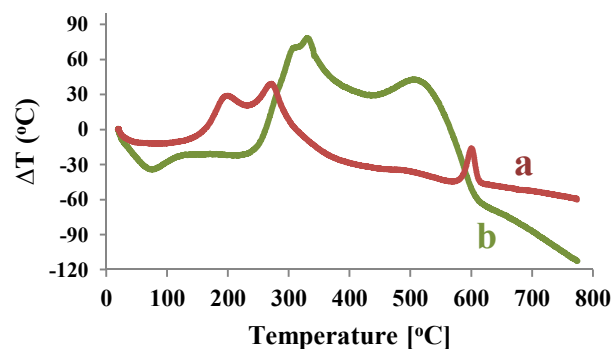


**Fig. 4** DTA curves of  $\text{Fe}_3\text{O}_4$  (a), and  $\text{Fe}_3\text{O}_4@SiO_2@chitosan$  (b).

Fig. 3b shows the TGA curve of  $\text{Fe}_3\text{O}_4@SiO_2@chitosan$  where two-stage weight loss is observed. The first stage below 250 °C resulted from the elimination of water on the surface of the polymer shell. The second stage is related to the decomposition of chitosan which started at 332 °C and completely burned out at 598 °C. Also, TGA curve indicates that the chitosan content of  $\text{Fe}_3\text{O}_4@SiO_2@chitosan$  is ~30.2%. Fig. 4 shows the DTA curves of  $\text{Fe}_3\text{O}_4$ , and  $\text{Fe}_3\text{O}_4@SiO_2@chitosan$ , which clearly shows the steps.

The SEM and TEM image of copper<sub>core</sub>silver<sub>shell</sub> nanoparticles immobilized on the yolk/shell  $\text{Fe}_3\text{O}_4@chitosan$ -derived carbon nanoparticle are shown in Fig. 5. The SEM images show uniform spherical particles (Fig. 5A and B). The TEM image clearly shows that  $\text{Fe}_3\text{O}_4$  was indeed coated by a layer of carbon nanoparticles (Fig. 5C). Three distinct components, the black cores of  $\text{Fe}_3\text{O}_4$ , the grey shells of carbon nanoparticle and the small black spheres of copper<sub>core</sub>silver<sub>shell</sub> nanoparticles, can be observed. The TEM image also shows that the metal nanoparticles with uniform size are densely distributed not only on the outer surface but also on the inner surface of carbonaceous shell. Moreover, the core/shell structure of copper<sub>core</sub>silver<sub>shell</sub> nanoparticles is clearly observable in Fig. 5D.

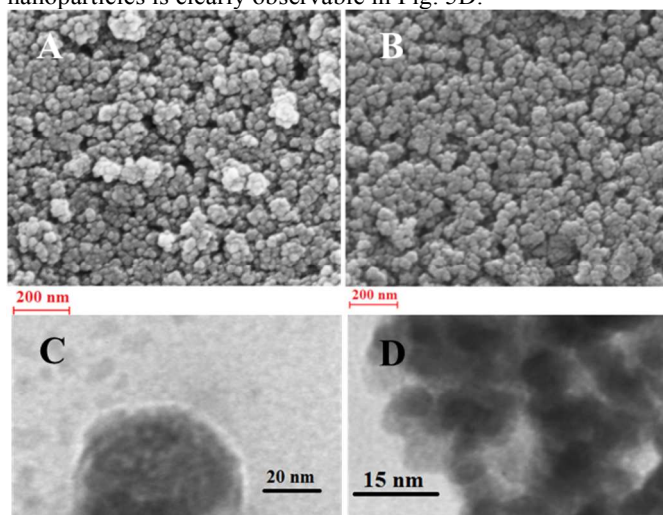


**Fig. 5** SEM (A, B) and TEM (C, D) images of  $\text{Cu}_{core}\text{Ag}_{shell}/\text{YS-Fe}_3\text{O}_4@(\text{Chit.der})\text{CNPs}$ .

XPS has often been employed for the surface characterization of various materials. So, to further analyze the  $\text{Cu}_{core}\text{Ag}_{shell}/\text{YS-}$

$\text{Fe}_3\text{O}_4@(\text{Chit.der})\text{CNPs}$  system, XPS was used to examine the composition of its surface (Fig. 6). The binding energy at 710.3 eV for Fe 2p cannot be observed, which further confirms that all the  $\text{Fe}_3\text{O}_4$  cores in the composite are confined within a shell of chitosan derived carbon nanoparticles/ $\text{Cu}_{\text{core}}\text{Ag}_{\text{shell}}$  (inset of Fig. 6). As shown in Fig. 6, the labelled peaks C 1s, N 1s, O 1s, Ag 3p, Ag 3d, and Cu 2p offer the accurate elemental composition of the prepared catalyst, which is in good accordance with the designation of the experiment. The absence of silicon band at around 104 eV confirms the selective etching of silica shell. Moreover, the XPS pattern shows the characteristic peaks of Cu and Ag with no indications for the presence of copper oxides. So, according to the results, Cu NPs

are really coated by a thin layer of silver. The UV-Vis absorption spectra of  $\text{Fe}_3\text{O}_4@(\text{Chit.der})\text{CNPs}$  and  $\text{Cu}_{\text{core}}\text{Ag}_{\text{shell}}/\text{YS-Fe}_3\text{O}_4@(\text{Chit.der})\text{CNPs}$  in water are illustrated in Fig. 6a and b, respectively. A broad featureless peak appears in the spectrum of core-shell  $\text{Fe}_3\text{O}_4@(\text{Chit.der})\text{CNPs}$  at a wavelength of about 395 nm. In the absorption spectrum of  $\text{Cu}_{\text{core}}\text{Ag}_{\text{shell}}/\text{YS-Fe}_3\text{O}_4@(\text{Chit.der})\text{CNPs}$ , the peak of Ag component appears at about 410 nm.

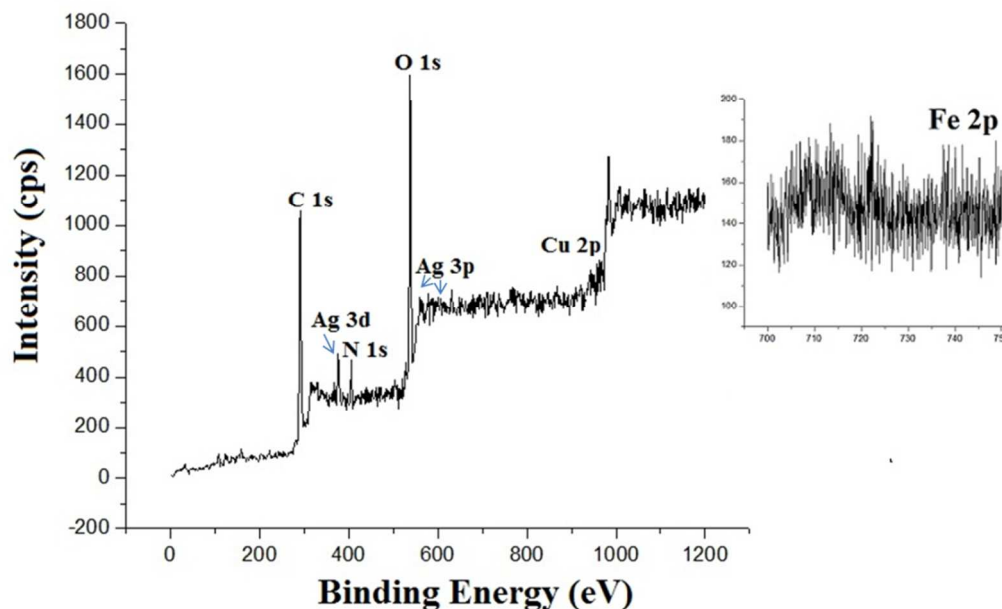


**Fig. 6** XPS full spectrum of  $\text{Cu}_{\text{core}}\text{Ag}_{\text{shell}}/\text{YS-Fe}_3\text{O}_4@(\text{Chit.der})\text{CNPs}$ , XPS high-resolution spectra of the Fe 2p of the as-prepared  $\text{Cu}_{\text{core}}\text{Ag}_{\text{shell}}/\text{YS-Fe}_3\text{O}_4@(\text{Chit.der})\text{CNPs}$  (inset).

The copper nanoclusters show no absorption band at greater than 300 nm but exhibit a monotonic spectrum rising exponentially toward shorter wavelengths.<sup>34</sup> The absence of observable absorption band at about 800 nm, which is attributed to the formation of copper oxide particles, demonstrates that the  $\text{Cu}_{\text{core}}\text{Ag}_{\text{shell}}$  nanoparticles were highly stable.

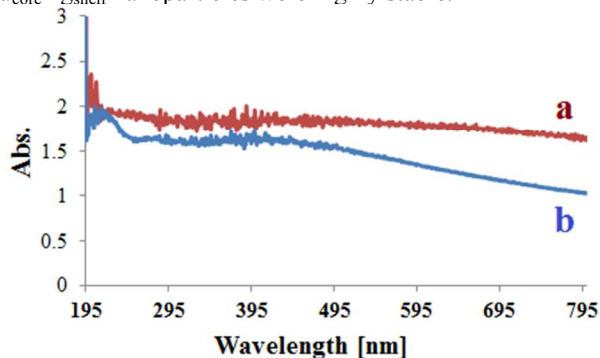


**Fig. 7** UV-Vis spectra of  $\text{Fe}_3\text{O}_4@(\text{Chit.der})\text{CNPs}$  (a) and  $\text{Cu}_{\text{core}}\text{Ag}_{\text{shell}}/\text{YS-Fe}_3\text{O}_4@(\text{Chit.der})\text{CNPs}$  (b).

EDS was used to measure the components of  $\text{Cu}_{\text{core}}\text{Ag}_{\text{shell}}/\text{YS-Fe}_3\text{O}_4@(\text{Chit.der})\text{CNPs}$  as shown in Figure 8. It is clear that the  $\text{Cu}_{\text{core}}\text{Ag}_{\text{shell}}/\text{YS-Fe}_3\text{O}_4@(\text{Chit.der})\text{CNPs}$  is composed of Fe, C, N, O, Ag and Cu elements. Appearance of Au element was due to the material coating by a layer of Au for EDS and SEM characterizations.

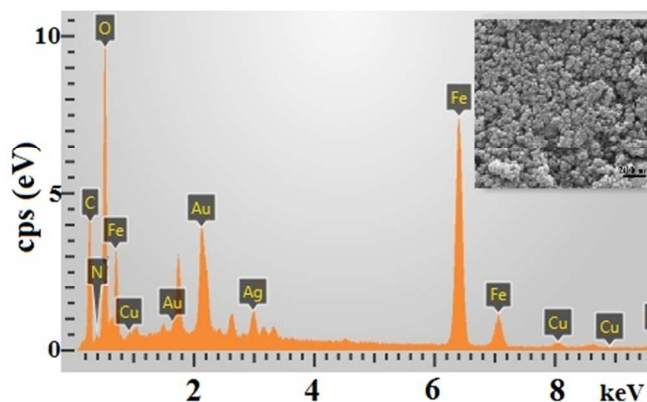


**Fig. 8** X-ray energy dispersive spectrum (EDS) of  $\text{Cu}_{\text{core}}\text{Ag}_{\text{shell}}/\text{YS-Fe}_3\text{O}_4@(\text{Chit.der})\text{CNPs}$ .

### The Catalytic activity of the Cu<sub>core</sub>Ag<sub>shell</sub>/YS-Fe<sub>3</sub>O<sub>4</sub>@(Chit.der)CNPs for epoxidation reaction of alkenes

Recently, reactions of water-insoluble organic compounds in aqueous suspensions ("on water") have received a great deal of attention,<sup>35,36</sup> which is due to their high efficiency and facile synthetic protocols. However, such reactions are still relatively unexplored. On the other hand, the development of the selective catalytic epoxidation pathways, without any radical initiators or reducing reagents, is highly desirable. So, in this work, the prepared catalyst was employed for the epoxidation reaction of alkenes on water with molecular oxygen as terminal oxidants.

Our investigation on the catalyst loading showed a high atom efficiency of title Cu<sub>core</sub>Ag<sub>shell</sub>/YS-Fe<sub>3</sub>O<sub>4</sub>@(Chit.der)CNPs. Only after 2 h, styrene converted completely using a low amount of catalyst (0.3 mol % Cu and 0.04 mol% Ag) and styrene oxide was obtained in 95% yield by an easy isolation with ethyl acetate as a safe solvent after removing the catalyst with an external magnetic field. More interestingly, the use of excess amount of styrene (1 mmol), rather than the catalyst (1×10<sup>-5</sup> mmol, 0.001 mol%) gave 51% epoxide yield after 28 h, indicating a high turnover number of 51000 for this nanostructured catalyst. Actually, due to the hydrophobic character of carbon nanoparticles in water medium the reactants tend to collect around carbon nanoparticles where the metal catalysts exist, so as a result of the existence of reactants and metal catalyst in the same region, an efficient catalytic reaction occurs. It is notable that when the catalyst was replaced by yolk/shell Fe<sub>3</sub>O<sub>4</sub>@chitosan/Cu<sub>core</sub>Ag<sub>shell</sub> composites, the

catalytic epoxidation reaction of styrene on water was accomplished in 5 h with 88% yield.

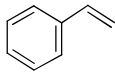
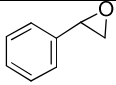
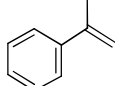
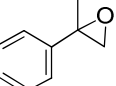
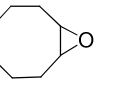
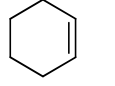
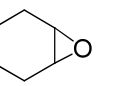
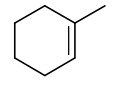
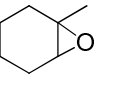
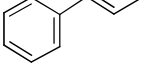
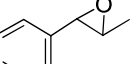
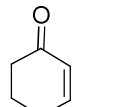
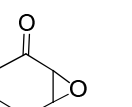
To investigate the effect of solvent, the epoxidation reaction of styrene as a model reaction was accomplished with different solvents and the conversion yields were measured by GC which the results are summarized in Table 1. According to these results, the best solvent was water which its effect was mentioned previously. Then, to evaluate the general applicability of the catalyst, different alkenes were tested for oxidation reaction using O<sub>2</sub> (1 atm) and 0.0005 g catalyst containing 0.3 mol % Cu and 0.04 mol% Ag at 25°C (Table 2).

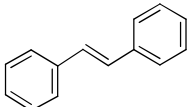
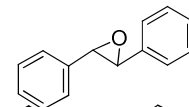
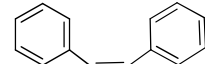
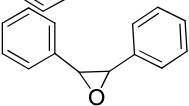
**Table 1** Influence of the different solvents on epoxidation reaction of styrene.<sup>a</sup>

Entry	Solvent	Conversion (%)
1	CH <sub>3</sub> CN	60
2	DMF	73
3	THF	54
4	Toluene	44
5	H <sub>2</sub> O	>99
6	EtOH	81

<sup>a</sup> Reaction conditions: 2 mL of solvent, 0.5 mmol alkene, O<sub>2</sub> (1 atm), and 0.0005 g catalyst at 25°C.

**Table 2** The epoxidation reaction of alkenes with Cu<sub>core</sub>Ag<sub>shell</sub>/YS-Fe<sub>3</sub>O<sub>4</sub>@(Chit.der)CNPs as catalyst.<sup>a</sup>

Entry	Compound	Product	Time (h)	Yield (%) <sup>b</sup>	Selectivity (%)
1			2	95	98
2			2.5	96	99
3			1.5	98	>99
4			1.8	97	>99
5			3	83	>99
6			4.5	79	>99
7			4	72	>99

8			4	61	>99
9			4	92	>99

<sup>a</sup> Reaction conditions: 2 mL of deionized water, 0.5 mmol alkene, O<sub>2</sub> (1 atm), and 0.0005 g catalyst at 25°C.

As can be seen, various alkenes can generate the related epoxides in good to excellent yields. The selectivities are given in Table 2 which showed that most of the alkenes only give the corresponding epoxide and only very low amount of benzaldehyde was detected due to ring opening reaction of styrene oxide (entry 1). Actually, the addition of copper in the bimetallic Cu-Ag catalyst increases the epoxidation selectivity with raising the relative difference between the barriers for the oxametallocycle ring-closure VS H-shift pathways, resulting in more epoxide formation.<sup>37</sup> It should be noted that that the catalyst was able to oxidize the tribstituted-, *E*-alkenes and also electron-deficient alkenes to the relevant epoxides in good yields (entries 5-8). In heterogeneous catalysis, considering the leaching of active metal species into solution is an important issue. So, to investigate it, in a separate experiment the catalyst was removed by the magnetic extraction after ~50% conversion under the reaction conditions. Then, the residue mixture was allowed to further treat under similar reaction conditions and the conversion yield was obtained by GC which showed the reaction did not proceed. Moreover, atomic absorption spectroscopy indicates that the metal content in the solution of the residue mixture is below the detection limit (0.1 ppm). According to these results, we conclude that metal leaching in the catalyst is negligible.

#### Recycling Cu<sub>core</sub>Ag<sub>shell</sub>/YS-Fe<sub>3</sub>O<sub>4</sub>@(Chit.der)CNPs

To investigate the productivity of the prepared catalyst, we examined the epoxidation reaction of styrene as a model reaction up to eight cycles after completion of the reaction. By design, the magnetic extraction eliminates the need for filtration or centrifugation and the workup of the final reaction mixture to recover the catalyst and consequently allows for easy recycling of the catalyst. The results are presented in Table 3 which indicate that the yield of product after every run does not change significantly. But, catalysis is a totally kinetic phenomenon and if a single data point was taken in each run after long reaction time, one might wrongly conclude that the catalyst is completely stable and recyclable. So, investigating the initial rates obtained from kinetic plots is a good approach to examine the recyclability and deactivation of the catalyst.<sup>38</sup> Therefore, the conversion yields for every run after 30 min for epoxidation reaction of styrene were measured (Table 3). As the conversion yields after 30 min for eight runs did not decrease significantly, we may conclude the good stability and recyclability of the synthesized catalyst.

The amounts of Cu<sub>core</sub>Ag<sub>shell</sub> after eight runs were measured with AAS to be 4.3% (w/w) Ag and 19.2% (w/w) Cu.

**Table 3** Effect of recycling on the catalytic activity and productivity of Cu<sub>core</sub>Ag<sub>shell</sub>/YS Fe<sub>3</sub>O<sub>4</sub>@(Chit.der)CNPs after 30 min (a) and after 2 h (b).<sup>a</sup>

No. of recycling steps	Conversion after 30 min <sup>b</sup> (%)	Conversion after 2 h <sup>b</sup> (%)
1	31	99
2	30	99
3	30	99
4	30	98
5	30	98
6	29	97
7	29	96
8	29	96

<sup>a</sup> Reaction conditions: 2 mL of deionized water, 0.5 mmol alkene, O<sub>2</sub> (1 atm), and 0.0005 g catalyst at 25°C.

#### Conclusion

Copper<sub>core</sub>Silver<sub>shell</sub> nanoparticles immobilized on the yolk/shell Fe<sub>3</sub>O<sub>4</sub>@chitosan-derived carbon nanoparticle were successfully synthesized and characterized. In this report, we have achieved several important objectives: i) Having a heterogeneous catalyst bearing the advantage of being magnetically separable and therefore removing the need of the catalyst filtration or centrifugation after completion of the reaction; ii) Employing hollow structure which has larger vacant space, lower density and higher surface area compared to the corresponding core-shell; iii) Using chitosan-derived carbon nanoparticles as really good candidates for stabilizing noble metals and heterogeneous catalysis due to the convenient method of synthesis, being biocompatible and inexpensive; iv) Due to the hydrophobic character of carbon nanoparticles, in water medium the reactants tend to collect around carbon nanoparticles where the metal catalyst exist, so because the reactants and metal catalyst are in the same region, efficient catalytic reaction occurs; v) Providing the catalyst contained Cu<sub>core</sub>Ag<sub>shell</sub> nanoparticles to have the optical and electric properties of both metals and also preventing the oxidation of the copper core. Moreover, Cu-Ag bimetallic catalyst is more selective than the pure silver toward epoxidation; and vi) Developing an efficient and green synthetic process for the facile and selective catalytic epoxidation of styrene.

#### Acknowledgements

We are grateful to Shahid Beheshti University Research Council for partial financial support of this work.

#### Notes and references

- <sup>a</sup> Faculty of Chemistry, Department of Polymer, Shahid Beheshti University, G.C., P.O. Box 1983963113 Tehran, Iran. Fax: +98 21 22431661; Tel: +98 21 29903102; E-mail: mnabid@sbu.ac.ir
1. N. Tian, Z.-Y. Zhou, S.-G. Sun, Y. Ding and Z. L. Wang, *Science*, 2007, **316**, 732-735.
  2. D. Astruc, *Nanoparticles and catalysis*, Wiley Online Library, 2008.
  3. V. Polshettiwar, R. Luque, A. Fihri, H. Zhu, M. Bouhrara and J.-M. Basset, *Chem. Rev.*, 2011, **111**, 3036-3075.
  4. A. Fihri, D. Cha, M. Bouhrara, N. Almana and V. Polshettiwar, *ChemSusChem*, 2012, **5**, 85-89.
  5. N. Madhavan, C. W. Jones and M. Weck, *Acc. Chem. Res.*, 2008, **41**, 1153-1165.
  6. S. Bhadra, B. Sreedhar and B. C. Ranu, *Adv. Synth. Catal.*, 2009, **351**, 2369-2378.
  7. Q. Yang, K. Y. Wang and T.-S. Chung, *Sep. Purif. Technol.*, 2009, **69**, 269-274.
  8. B. Dai, M. Cao, G. Fang, B. Liu, X. Dong, M. Pan and S. Wang, *J. Hazard. Mater.*, 2012, **219-220**, 103-110.
  9. M. Rana, M. Halim, S. Safiullah, M. M. Mollah, M. Azam, M. Goni, M. K. Hossain and M. Rana, *J. Appl. Sci.*, 2009, **9**, 2762-2769.
  10. S. R. Hall, A. M. Collins, N. J. Wood, W. Ogasawara, M. Morad, P. J. Miedziak, M. Sankar, D. W. Knight and G. J. Hutchings, *RSC Adv.*, 2012, **2**, 2217-2220.
  11. M. G. Dekamin, M. Azimoshan and L. Ramezani, *Green Chem.*, 2013, **15**, 811-820.
  12. M. P. Sk, A. Jaiswal, A. Paul, S. S. Ghosh and A. Chattopadhyay, *Scientific reports*, 2012, **2**.
  13. A. Jaiswal, S. S. Ghosh and A. Chattopadhyay, *Chem. Commun.*, 2012, **48**, 407-409.
  14. H. Li, X. He, Z. Kang, H. Huang, Y. Liu, J. Liu, S. Lian, C. H. A. Tsang, X. Yang and S. T. Lee, *Angew. Chem. Int. Ed.*, 2010, **49**, 4430-4434.
  15. R. Güttel, M. Paul and F. Schüth, *Catal. Sci. Tech.*, 2011, **1**, 65-68.
  16. C. C. Yec and H. C. Zeng, *Chem. Mater.*, 2012, **24**, 1917-1929.
  17. Y. Chen, Y. Gao, H. Chen, D. Zeng, Y. Li, Y. Zheng, F. Li, X. Ji, X. Wang and F. Chen, *Adv. Funct. Mater.*, 2012, **22**, 1586-1597.
  18. T. Yang, J. Liu, Y. Zheng, M. J. Monteiro and S. Z. Qiao, *Chem. Eur. J.*, 2013, **19**, 6942-6945.
  19. Y. Chen, H. Chen, M. Ma, F. Chen, L. Guo, L. Zhang and J. Shi, *J. Mater. Chem.*, 2011, **21**, 5290-5298.
  20. H. Wu, G. Liu, S. Zhang, J. Shi, L. Zhang, Y. Chen, F. Chen and H. Chen, *J. Mater. Chem.*, 2011, **21**, 3037-3045.
  21. M. R. Nabid and S. J. Tabatabaei Rezaei, *Appl. Catal. A: Gen.*, 2009, **366**, 108-113.
  22. M. R. Nabid, Y. Bide and S. J. Tabatabaei Rezaei, *Appl. Catal. A: Gen.*, 2011, **406**, 124-132.
  23. M. R. Nabid, Y. Bide and M. Niknezhad, *ChemCatChem*, 2014, **6**, 538-546.
  24. M. R. Nabid and Y. Bide, *Appl. Catal. A: Gen.*, 2014, **469**, 183-190.
  25. M. Nabid, Y. Bide, E. Aghaghafari and S. Rezaei, *Catal. Lett.*, 2014, **144**, 355-363.
  26. H. Ahmar, A. R. Fakhari, M. R. Nabid, S. J. T. Rezaei and Y. Bide, *Sens. Actuators, B*, 2012, **171**, 611-618.
  27. S. Gangopadhyay, G. Hadjipanayis, B. Dale, C. Sorensen, K. Klabunde, V. Papaefthymiou and A. Kostikas, *Phys. Rev. B: Condens. Matter*, 1992, **45**, 9778.
  28. R. Seshadri, R. Sen, G. Subbanna, K. Kannan and C. Rao, *Chem. Phys. Lett.*, 1994, **231**, 308-313.
  29. M. Grouchko, A. Kamyshny and S. Magdassi, *J. Mater. Chem.*, 2009, **19**, 3057-3062.
  30. J. T. Jankowiak and M. A. Barteau, *J. Catal.*, 2005, **236**, 366-378.
  31. J. Liu, Z. Sun, Y. Deng, Y. Zou, C. Li, X. Guo, L. Xiong, Y. Gao, F. Li and D. Zhao, *Angew. Chem. Int. Ed.*, 2009, **48**, 5875-5879.
  32. H. Deng, X. Li, Q. Peng, X. Wang, J. Chen and Y. Li, *Angew. Chem. Int. Ed.*, 2005, **44**, 2782-2785.
  33. Y. Yang, J. Cui, M. Zheng, C. Hu, S. Tan, Y. Xiao, Q. Yang and Y. Liu, *Chem. Commun.*, 2012, **48**, 380-382.
  34. M. Zhao, L. Sun and R. M. Crooks, *J. Am. Chem. Soc.*, 1998, **120**, 4877-4878.
  35. B. K. Price and J. M. Tour, *J. Am. Chem. Soc.*, 2006, **128**, 12899-12904.
  36. A. El-Batta, C. Jiang, W. Zhao, R. Anness, A. L. Cooksy and M. Bergdahl, *J. Org. Chem.*, 2007, **72**, 5244-5259.
  37. J. T. Jankowiak and M. A. Barteau, *J. Catal.*, 2005, **236**, 379-386.
  38. C. W. Jones, *Top. Catal.*, 2010, **53**, 942-952.